Disc vs. Annulus: On the Bleaching Pattern Optimization for FRAP Experiments

Ctirad Matonoha[1(✉)], Štěpán Papáček[2], and Stefan Kindermann[3]

[1] Institute of Computer Science, The Czech Academy of Sciences,
Pod Vodárenskou věží 2, 182 07 Prague 8, Czech Republic
matonoha@cs.cas.cz
[2] Institute of Complex Systems, South Bohemian Research Center of Aquaculture and Biodiversity of Hydrocenoses, Faculty of Fisheries and Protection of Waters, University of South Bohemia in České Budějovice,
Zámek 136, 373 33 Nové Hrady, Czech Republic
[3] Industrial Mathematics Institute, University of Linz,
Altenbergerstr. 69, 4040 Linz, Austria

Abstract. This study deals with the problem of optimal setting of experimental design variables, which controls the accuracy of the numerical process of determining model parameters from data. Our approach, although case independent, is formulated as an inverse problem of a diffusion coefficient estimation using the FRAP (Fluorescence Recovery After Photobleaching) experimental technique. The key concept relies on the analysis of the sensitivity of the measured output with respect to the model parameters. Based on this idea, we optimize an experimental design factor being the initial concentration of some particles. Numerical experiments on a 2D finite domain show that the discretized optimal initial condition attains only two values representing the existence or non-existence of diffusive particles. The number of jumps between these values determines the connectivity (or the bleaching pattern) and is dependent on the value of a diffusion coefficient, e.g., the annulus shaped initial condition is better than a disc for some specific range of model parameters.

Keywords: Optimization · Parameter identification · FRAP
Bleaching pattern · Initial boundary value problem
Sensitivity measure

1 Introduction

The continuous enhancement and sophistication of experimental devices in service of biological community take advantage of the fast development of informatics and image processing. However, it is not a rare case that a large amount of spatio-temporal data, e.g., in form of a time sequence of images, is routinely generated without a clear idea about further data processing.

T. Kozubek et al. (Eds.): HPCSE 2017, LNCS 11087, pp. 160–173, 2018.
https://doi.org/10.1007/978-3-319-97136-0_12

The aim of this paper is to (re)establish the link between experimental conditions (experimental protocol) and the accuracy of the resulting data processing. Our simplified case study on FRAP (Fluorescence Recovery After Photobleaching) data processing [6,14] serves as a paradigmatic example of the inverse problem of the diffusion parameter estimation from spatio-temporal measurements of fluorescent particle concentration. The FRAP technique is based on measuring the fluorescence intensity (proportional to non-bleached particles concentration) in a region of interest (being usually an Euclidian 2D domain) in response to a high-intensity laser pulse. The laser pulse (the so-called *bleach*) causes an irreversible loss in fluorescence of some particles residing originally in the bleached area, presumably without any damage to intracellular structures. After the bleach, we observe the change in fluorescence intensity in a monitored region reflecting the diffusive transport of fluorescent particles from the area outside the bleach [12,17].

A natural question is how the experimental settings influence the accuracy of the resulting parameter estimates. There are many rather empirical recommendations related to the design of a photobleaching experiment, e.g., the bleach spot shape and size [2], the region of interest (its location and size), or the total time of measurement, see [16] and references within. However, we would have a more rigorous tool for the choice of experimental design factors. This is because the setting of initial conditions of an experiment not only influences the following data measurement process. There is somewhat hidden a related data processing part. Mainly in case of a model-based design of experiments and when the measured data are used in the frame of an inverse problem of model parameter estimation. Having a reliable process model, e.g. [11], we can perform the subsequent sensitivity analysis with respect to the model parameters [3]. Consequently, we are allowed to formulate the problem as the maximization of a sensitivity measure leading to the optimal initial condition (an optimal bleaching pattern).

The paper is organized as follows. In Sect. 2, we introduce the problem, define the sensitivity measure and formulate the optimization problem. Section 3 describes some numerical issues of sensitivity measure evaluation. In Sect. 4, we provide a numerical example to show that our theoretical basis is well founded and that the optimal initial condition strongly depends on the diffusion coefficient and leads to a variety of bleaching patterns. Finally, some conclusions are presented in Sect. 5.

2 Problem Formulation

Let us consider the Fickian diffusion with a *constant* diffusion coefficient $D > 0$ and assume a spatially radially symmetric observation domain, i.e., the data are observed on a cylinder with the radius R and height T [8]. Taking into account the usual case of radial symmetry of the FRAP experiment, the simplest governing equation for the spatio-temporal distribution of fluorescent particle concentration $u(r, t)$ is the diffusion equation as follows

$$\frac{\partial u}{\partial t} = D\left(\frac{\partial^2 u}{\partial r^2} + \frac{1}{r}\frac{\partial u}{\partial r}\right), \tag{1}$$

where $r \in (0, R]$, $t \in [0, T]$, with the initial and Neumann boundary conditions

$$u(r, 0) = u_0(r), \quad \frac{\partial u}{\partial r}(R, t) = 0. \tag{2}$$

We consider the diffusion equation in polar coordinates since both the whole boundary value problem and the bleaching pattern used in FRAP experiments have the rotational (radial) symmetry.[1]

The main issue in FRAP and related inverse problems of parameter estimation is to find the value of the underlying model parameters (e.g., the diffusion coefficient D) from spatio-temporal measurements of the concentration $u(r, t)$, see [13,14].

Obviously, the measured data are discrete and each data entry quantifies the variable u at a particular spatio-temporal point (r, t) in a finite domain, i.e.,

$$u(r_i, t_j) \in [0, u_{max}], \quad i = 0 \ldots n, \quad j = 0 \ldots m,$$

where i is the spatial index uniquely identifying the pixel position where the value of fluorescence intensity u is measured and j is the time index (the initial condition corresponds to $j = 0$). Usually, the data points are uniformly distributed both in time (the time interval Δt between two consecutive measurements is constant) and space, i.e., on an equidistant mesh with the step-size Δr, see [8]. Having $N_{\text{data}} := (m + 1) \times (n + 1)$ the total number of spatio-temporal data points, we can define a forward map (also called a parameter-to-data map)

$$\begin{aligned} F : \mathcal{R} &\to \mathcal{R}^{N_{\text{data}}} \\ (D) &\to u(r_k, t_k)_{k=1}^{N_{\text{data}}}. \end{aligned} \tag{3}$$

Our regression model is now

$$F(D) = u_e, \tag{4}$$

where the data $u_e \in \mathcal{R}^{N_{\text{data}}}$ are modeled as contaminated with additive white noise

$$u_e = F(D_T) + e = u(r_k, t_k)_{k=1}^{N_{\text{data}}} + (e_k)_{k=1}^{N_{\text{data}}}. \tag{5}$$

Here D_T denotes the true coefficient and $e \in \mathcal{R}^{N_{\text{data}}}$ is a data error vector, which we assume to be normally distributed with variance σ^2 for each time instant t_j, i.e., $e_j = \mathcal{N}(0, \sigma^2)$, $j = 0, \ldots, m$, $e_j \in \mathcal{R}^{n+1}$.

Given some data, the aim of the parameter estimation problem is to find D_T, such that Eq. (4) is satisfied in some appropriate sense. Since Eq. (4) usually consists of an overdetermined system (there are more data points than unknowns), it cannot be expected that it holds with equality, but instead an appropriate notion of a solution is that of a least-squares solution D_c (with $\| \cdot \|$ denoting the Euclidean norm on $\mathcal{R}^{N_{\text{data}}}$):

$$\| u_e - F(D_c) \|^2 = \min_{D>0} \| u_e - F(D) \|^2 . \tag{6}$$

[1] In our preceding papers [6–8,14], we employed the Cartesian coordinate system.

Remark 1. The above defined parameter identification problem (6) is usually ill-posed (in a Hadamard sense) for non-constant coefficients [5] and a regularization technique has to be employed. Let us state, that the theory of regularization of ill-posed problems is well developed, see [4] and references within there. For some practical examples related to FRAP data processing see our works [6,7, 14]. However, if we a-priori restrict the coefficients D to be constant, then the identification problem becomes well-posed.

Having the noisy data as in (5), the estimated value D_c of the true diffusion coefficient D_T can be computed numerically by solving the inverse problem to initial boundary value (IBV) problems (1)–(2). It can be shown [1,3,8], that for our case of single scalar parameter estimation and white noise as data error assumed, the expected relative error in D_T depends on the data noise level and a factor, which we call the global semi-relative squared sensitivity S_{GRS}, as follows

$$\mathbb{E}\left(\left|\frac{D_c - D_T}{D_T}\right|^2\right) \sim \frac{\sigma^2}{S_{GRS}}, \tag{7}$$

where $\mathbb{E}$ is the expected value and σ^2 denotes the variance of the additive Gaussian noise. The sensitivity measure S_{GRS}, that depends on the initial condition u_0, is defined on a spatio-temporal mesh by

$$S_{GRS}(u_0) = D_T^2 \sum_{i=0}^{n} \sum_{j=1}^{m} \left[\frac{\partial}{\partial D} u(r_i, t_j)|_{D=D_T}\right]^2, \tag{8}$$

where $\frac{\partial}{\partial D} u(r_i, t_j)$ is the usual sensitivity of the model output at the spatio-temporal point (r_i, t_j) with respect to the parameter D.

It is obvious from this estimate that if the noise level is fixed, the estimation of D_T can only be improved by switching to an experimental design with a higher sensitivity. The sensitivity measure (8) involves several design parameters. If the spatio-temporal grid for the data measurement is given, i.e., all the above parameters $R, T, \Delta r, \Delta t$ are fixed, there is only one way to maximize the sensitivity measure S_{GRS}: to consider the *initial condition* u_0 in (2) as the experimental design parameter. It means, for the discretized version of the IBV problems (1)–(2), the aim is to find the initial condition $(u_{00}, \ldots, u_{0n})^T = (u_0(r_0), \ldots, u_0(r_n))^T \in \mathcal{R}^{n+1}$ such that S_{GRS} is maximized and hence the expected error in D_T is minimized. In order to do so, we establish the bounds where the initial condition is considered: $\underline{u_0} \le u_{0i} \le \overline{u_0}$, $i = 0, \ldots, n$, where $\underline{u_0}, \overline{u_0} \in \mathcal{R}$, $\underline{u_0} < \overline{u_0}$. The optimization problem is formulated as follows

$$u_0^{opt} = \arg \max_{u_0 \in \mathcal{R}^{n+1}} S_{GRS}(u_0) \quad \text{subject to} \quad \underline{u_0} \le u_{0i} \le \overline{u_0}, \quad i = 0, \ldots, n. \tag{9}$$

Without loss of generality, we set $\underline{u_0} = 0$ (zero components) and $\overline{u_0} = 1$ (non-zero components).

3 Numerical Issues of Sensitivity Measure (8) evaluation

Based on the previously fixed parameters R, T, it is convenient to introduce the following scaling of the space and time coordinates and to define a scaled diffusion coefficient δ

$$\tilde{r} := \frac{r}{R}, \quad \tilde{t} := \frac{t}{T}, \quad \delta := \frac{DT}{R^2}. \tag{10}$$

Instead of the Fick diffusion Eq. (1), the concentration u, in the scaled coordinates $\tilde{r}, \tilde{t}$, then satisfies the equation

$$\frac{\partial u}{\partial \tilde{t}} = \delta \left(\frac{\partial^2 u}{\partial \tilde{r}^2} + \frac{1}{\tilde{r}} \frac{\partial u}{\partial \tilde{r}} \right), \tag{11}$$

where $\tilde{r} \in (0, 1]$, $\tilde{t} \in [0, 1]$, with the initial and Neumann boundary conditions

$$u(\tilde{r}, 0) = u_0(\tilde{r}), \quad \frac{\partial u}{\partial \tilde{r}}(1, \tilde{t}) = 0. \tag{12}$$

Let us fix $n+1$ as a number of spatial points and $m+1$ as a number of time measurements. Consider a spatio-temporal grid $\{\tilde{r}_i, \tilde{t}_j\}$, $i = 0 \dots n$, $j = 0 \dots m$, where $\tilde{r}_0 = 0$, $\tilde{r}_n = 1$, $\tilde{t}_0 = 0$, $\tilde{t}_m = 1$, with corresponding spatial and time steps $\Delta\tilde{r} = \frac{1}{n}$ and $\Delta\tilde{t} = \frac{1}{m}$, respectively. Consequently, $u(\tilde{r}_i, 0) = u_0(\tilde{r}_i)$, $i = 0 \dots n$, represents the initial condition (evaluated at discrete points $\tilde{r}_i$) and $\frac{\partial u}{\partial \tilde{r}}(1, \tilde{t}_j) = 0$, $j = 1 \dots m$, represents the homogeneous Neumann boundary condition.

We use the finite difference Crank-Nicolson scheme to compute a numerical solution $u_{i,j} := u(\tilde{r}_i, \tilde{t}_j)$, $i = 0 \dots n-1$, $j = 1 \dots m$, of the IBV problems (11)–(12). After some algebraic manipulation we arrive at a linear system with a three-diagonal symmetric positive definite matrix

$$(\gamma^+ Z - hS) u_{\cdot,j} = (\gamma^- Z + hS) u_{\cdot,j-1} \tag{13}$$

for $(u_{0,j}, \dots, u_{n-1,j})^T$. The Neumann boundary condition implies $u_{n,j} = u_{n-1,j}$. Here

$$S = \begin{bmatrix} 0 & s_0 & & & & \\ s_0 & 0 & s_1 & & & \\ & s_1 & 0 & s_2 & & \\ & & \ddots & \ddots & \ddots & \\ & & & s_{n-3} & 0 & s_{n-2} \\ & & & & s_{n-2} & s_{n-1} \end{bmatrix},$$

$$h = \frac{\Delta\tilde{t}}{\Delta\tilde{r}}, \quad \gamma^+ = \frac{\Delta\tilde{r}}{\delta} + h, \quad \gamma^- = \frac{\Delta\tilde{r}}{\delta} - h, \quad s_k = \frac{2k+1}{4}, \ k = 0, \dots, n-1,$$

$$Z = \mathrm{diag}(\tfrac{1}{4}, 1, 2, \dots, n-2, n-1).$$

The formula (8) for S_{GRS} involves the derivative of the solution $u(r, t)$ of (1)–(2) with respect to the diffusion parameter D. Taking the scaled variables (10) and using the derivative of a composite function, we find that

$$D\frac{\partial u}{\partial D} = D\frac{\partial u}{\partial \delta}\frac{\partial \delta}{\partial D} = \frac{DT}{R^2}\frac{\partial u}{\partial \delta} = \delta\frac{\partial u}{\partial \delta} = \delta\frac{\partial u}{\partial \tilde{t}}\frac{\partial \tilde{t}}{\partial \delta} = -\frac{Dt}{\delta R^2}\frac{\partial u}{\partial \tilde{t}} = -\tilde{t}\frac{\partial u}{\partial \tilde{t}}.$$

Thus, the scaled sensitivity measure (8) has the form

$$S_{GRS} = \delta_T^2 \sum_{i=0}^{n} \sum_{j=1}^{m} \left[\frac{\partial}{\partial \delta} u(\tilde{r}_i, \tilde{t}_j)|_{\delta=\delta_T} \right]^2 = \sum_{i=0}^{n} \sum_{j=1}^{m} \left[\tilde{t}_j \frac{\partial}{\partial \tilde{t}} u(\tilde{r}_i, \tilde{t})|_{\tilde{t}=\tilde{t}_j} \right]^2. \quad (14)$$

Replacing the derivative with a finite difference, and using the fact that $\tilde{t}_j = j\Delta\tilde{t}$, the sensitivity measure S_{GRS} can be approximated as follows

$$\begin{aligned} S_{GRS}(u_0) &\approx \sum_{i=0}^{n} \sum_{j=1}^{m} \left[j\Delta\tilde{t} \, \frac{u(\tilde{r}_i, \tilde{t}_j) - u(\tilde{r}_i, \tilde{t}_{j-1})}{\Delta\tilde{t}} \right]^2 \\ &= \sum_{j=1}^{m} j^2 \sum_{i=0}^{n} \left[u_{i,j} - u_{i,j-1} \right]^2 =: S_{app}(u_0(\tilde{r})), \end{aligned} \quad (15)$$

where the values $u_{i,j}$ are computed from $u_{i,j-1}$ using (13), thus no extra work is necessary.

As we already proved in [9], the components of the vector u_0^{opt} (in discrete points $\tilde{r}_0, \ldots, \tilde{r}_n$) attain only two values $\underline{u_0}$ and $\overline{u_0}$. The jumps between these values in fact represent the discontinuities in bleached domain leading to more complex bleaching patterns, see [9] for more details.

Remark 2. A variety of patterns arises as optimal for slow diffusive transport (for low values of δ), e.g., the bleaching pattern is called a *disc*, an *annulus*, a *disc & annulus*, or an *annulus & annulus* if

$$\begin{aligned} u_0^{opt} &= [\overline{u_0}, \ldots, \overline{u_0}, \underline{u_0}, \ldots, \underline{u_0}]^T, \\ u_0^{opt} &= [\underline{u_0}, \ldots, \underline{u_0}, \overline{u_0}, \ldots, \overline{u_0}, \underline{u_0}, \ldots, \underline{u_0}]^T, \\ u_0^{opt} &= [\overline{u_0}, \ldots, \overline{u_0}, \underline{u_0}, \ldots, \underline{u_0}, \overline{u_0}, \ldots, \overline{u_0}, \underline{u_0}, \ldots, \underline{u_0}]^T, \\ u_0^{opt} &= [\underline{u_0}, \ldots, \underline{u_0}, \overline{u_0}, \ldots, \overline{u_0}, \underline{u_0}, \ldots, \underline{u_0}, \overline{u_0}, \ldots, \overline{u_0}, \underline{u_0}, \ldots, \underline{u_0}]^T, \end{aligned}$$

respectively, see Fig. 1. Note that this formulation is well suited for both (i) the optimization of size of a specific bleached domain geometry (shape or pattern), and (ii) the optimization between all possible patterns (as explained above).

4 Bleaching Pattern Optimization for FRAP Experiments

Previously, in [15], we found that there exists an optimal size of the bleached domain when the pattern is restricted to the simply connected (disc) shape only. The quantitative aspect of our result announced in [15], i.e., $r_{opt} = 1.728\sqrt{D_c T}$, valid for an infinite domain, was confirmed once again in this study, see Fig. 2. Indeed, comparing two cases with $D = 0.1$ (the dashed curve) and $D = 0.001$ (the dotted curve), we see that the optimal disc radius with 100 times lower diffusive mobility is 10 times smaller. Here, we have numerically (for $T = 1$), $r_{opt} = 0.56$ and $r_{opt} = 0.06$, for $\mathrm{D} = 0.1$ and $\mathrm{D} = 0.001$, respectively; while the

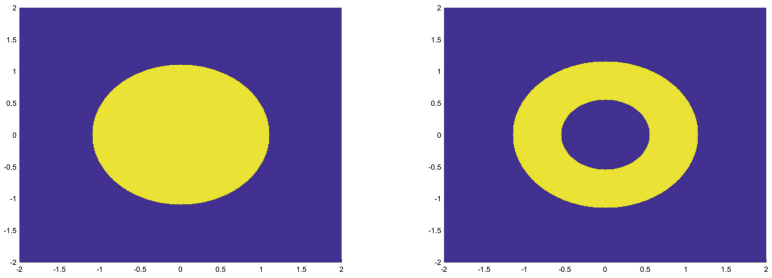

Fig. 1. Optimal pattern of initial bleach for two different values of $\delta = \frac{DT}{R^2}$, see [9]. Left: $\delta = 1/4$ (*disc*), right: $\delta = 1/12$ (*annulus*).

"analytical formula" according to [15] leads to values $r_{opt(D=0.1)} = 0.546$ and $r_{opt(D=0.001)} = 0.055$, respectively.

In our work [9], we found various optimal initial conditions for an inverse problem of diffusion constant estimation on an infinite two-dimensional domain. An interesting pattern of increasingly complicated (with respect to connectivity) optimal initial shapes was discovered by an efficient algorithm of numerical optimization. Figure 1 shows the result for two values of dimensionless diffusion constant δ. The exhaustive explanation of such an interesting result is far of scope of this paper. Nevertheless, the principal cause behind this phenomenon is clear: with the restricted observation domain and fixed overall measurement time interval, the more complex pattern provides a better exploitation of spatio-temporal data because the sensitivity measure S_{GRS}, see (8), gives a higher value than for any simpler shape, e.g., a disc (common bleaching shape used in FRAP community).

As follows, we present a numerical case study related to the FRAP experiment on a finite domain (with the Neumann homogeneous boundary condition) when the bleaching pattern (or shape) is not restricted previously. The goal is twofold: (i) to demonstrate (once again) the influence of S_{app} on a solution of inverse problem (6), and (ii) to show the unexpected variety of patterns corresponding to optimal initial conditions, see Fig. 1.

Further, in order to perform our virtual FRAP experiments (getting several sets of virtual experimental data), we used two values of $D = D_T$ and two levels of noise σ. The parameters defining the experimental protocol were fixed, more specifically:

$$R = 1, \quad T = 1, \quad n = 100, \quad m = 300.$$

The sequence of numerical computation is the following:

1. Choose a diffusion coefficient D_T and the non-zero components of $u_0 \in \mathcal{R}^{n+1}$.
2. Generate the time evolution $u_{i,j}$ computed using (13).
3. Produce the noisy data from $u_{i,j}$ using (5).
4. Solve problem (6) and find a solution D_c.

Figure 3 shows illustrative examples of exact and noisy data, which represents a time sequence of "row" data for further processing. The dashed lines are the

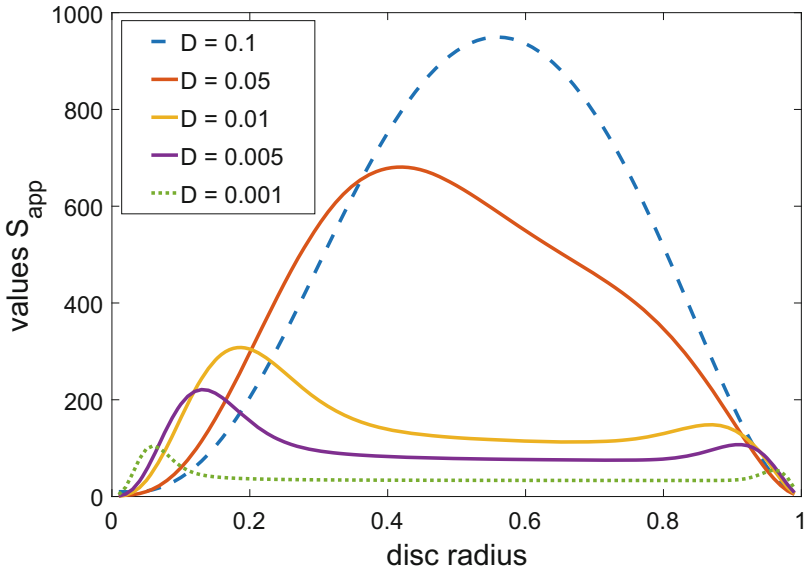

Fig. 2. The values S_{app} vs. disc radius r for 5 different diffusion coefficients D. The existence of optimal disc radii for each case is clearly visible.

initial conditions u_0 ($j = 0$) and the solid lines from top to bottom correspond to every 30-th time instant of exact data, i.e., for $j = 30, 60, \ldots, 300$. The noisy data are plotted only for $j = 0, 150, 300$. The known values of D_T and σ were used only *a posteriori* for the evaluation of relative error $\mathbb{E}$ and value $\frac{\sigma^2}{S_{app}}$, cf. (7), used in Figs. 4 and 5.

In order to generate our virtual "row" data, we used several following different initial conditions $u_0 \in \mathcal{R}^{101}$ with non-zero components u_{0i}, $i \in \{0, \ldots, 100\}$, listed below, with corresponding values of S_{app}. For the first set of initial conditions IC1–IC5 the value $D_T = 0.1$ was used (with two levels of the noise $\sigma = 0.01$ and $\sigma = 0.1$), while for the second set of initial conditions IC6-IC9 we chose the slower diffusion $D_T = 0.01$ (and both levels of the noise) in order to allow a more complicated bleaching pattern as optimal.

The first set of initial conditions for $D_T = 0.1$:

- IC1: u_0 has non-zero components for $i = 0, \ldots, 55 \quad \Rightarrow \quad S_{app} = 949.5$ (maximal value of S_{app} among all discs)
- IC2: u_0 has non-zero components for $i = 19, \ldots, 51 \quad \Rightarrow \quad S_{app} = 589.2$ (the initial condition leading to maximal value of S_{app} among all annuli in case of using another value $D_T = 0.01$)
- IC3: u_0 has non-zero components for $i = 0, \ldots, 79 \quad \Rightarrow \quad S_{app} = 516.7$ (suboptimal disc of a large radius)
- IC4: u_0 has non-zero components for $i = 0, \ldots, 29 \quad \Rightarrow \quad S_{app} = 478.9$ (suboptimal disc of a small radius)

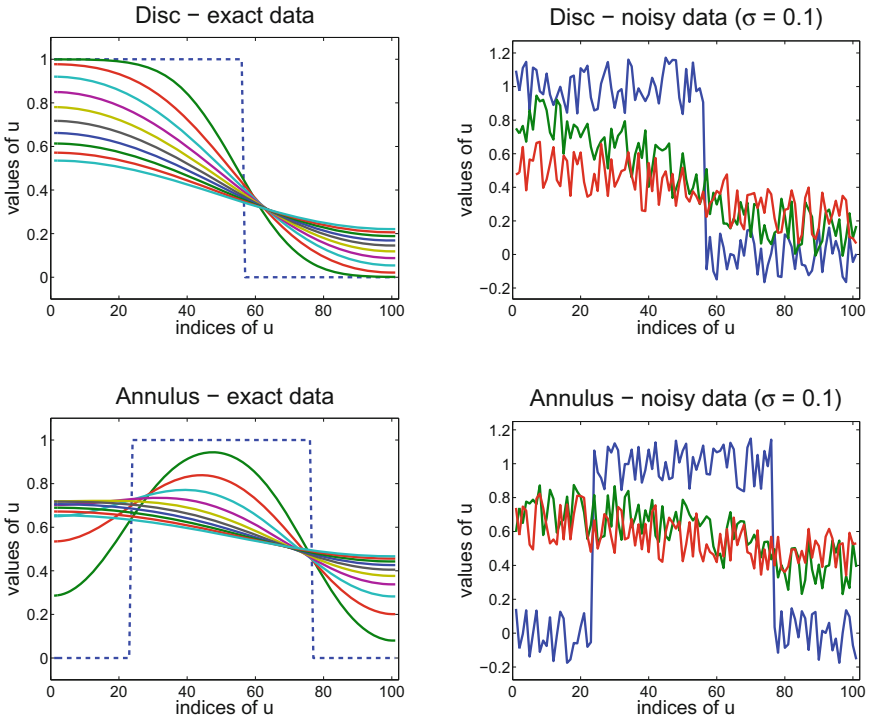

Fig. 3. Initial values of u_0 (the dashed stepwise curve) and the time evolution of the solution u_{ij} computed using (13) for $D_T = 0.1$. On top: disc – the non-zero components of u_0 have indices $i = 0, \ldots, 55$. Beneath: annulus – the non-zero components of u_0 have indices $i = 23, \ldots, 75$. Left: exact data. Right: corresponding noisy data with $\sigma = 0.1$.

– IC5: u_0 has non-zero components for $i = 44, \ldots, 55 \quad \Rightarrow \quad S_{app} = 100.5$ (suboptimal annulus).

The second set of initial conditions for $D_T = 0.01$:

– IC6: u_0 has non-zero components for $i = 19, \ldots, 51 \quad \Rightarrow \quad S_{app} = 458.5$ (maximal value of S_{app} among all annuli)
– IC7: u_0 has non-zero components for $i = 0, \ldots, 18 \quad \Rightarrow \quad S_{app} = 307.7$ (maximal value of S_{app} among all discs)
– IC8: u_0 has non-zero components for $i = 42, \ldots, 69 \quad \Rightarrow \quad S_{app} = 305.2$ (suboptimal annulus)
– IC9: u_0 has non-zero components for $i = 0, \ldots, 57 \quad \Rightarrow \quad S_{app} = 115.7$ (suboptimal disc).

Remark 3. It could be objected that the optimal annulus is missing among the initial conditions IC1–IC5. This is true and the reason is simple. In case a disc is the optimal bleaching pattern, the optimal annulus ends at the domain boundary.

The proof relies on the evaluation of S_{GRS} (and obviously S_{app}, as well), which leads to the identical results, cf. (14). This kind of "impure" annuli will be excluded. Note that in case of a "pure annulus" as the optimal bleaching pattern, the "complement" is the combination of a disc and "impure" annulus. The reason why to exclude the bleaching domain from the border region as well as the detailed analysis of the phenomenon of spurious optima is left to the near future.

The sensitivity measure S_{app}, computed from exact data (without noise), was used for determining the values $\frac{\sigma^2}{S_{app}}$ which theoretically give the upper bound on the expected value $\mathbb{E}$, see (7). In Tables 1–2, we resume the theoretical values of expected relative errors of a diffusion constant estimate, see (7), for all initial conditions (IC1–IC9) and both levels of noise (18 quantities in total).

Table 1. Expected values $\frac{\sigma^2}{S_{app}}$ for initial conditions IC1–IC5 (with $D_T = 0.1$) defining the concentration $u_0(r_i)$. Two levels of noise are defined by σ.

IC	IC1	IC2	IC3	IC4	IC5
S_{app}	949.5	589.2	516.7	478.9	100.5
σ	0.01	0.01	0.01	0.01	0.01
σ^2/S_{app}	1.05E–7	1.70E–7	1.94E–7	2.09E–7	9.95E–7
σ	0.1	0.1	0.1	0.1	0.1
σ^2/S_{app}	1.05E–5	1.70E–5	1.94E–5	2.09E–5	9.95E–5

Table 2. Expected values $\frac{\sigma^2}{S_{app}}$ for initial conditions IC6–IC9 (with $D_T = 0.01$) defining the concentration $u_0(r_i)$. Two levels of noise are defined by σ.

IC	IC6	IC7	IC8	IC9
S_{app}	458.5	307.7	305.2	115.7
σ	0.01	0.01	0.01	0.01
σ^2/S_{app}	2.18E–7	3.25E–7	3.28E–7	8.64E–7
σ	0.1	0.1	0.1	0.1
σ^2/S_{app}	2.18E–5	3.25E–5	3.28E–5	8.64E–5

The 18 data sets defined by 9 different initial bleaching patterns IC1–IC9 and two noise levels were further processed and compared mutually. That is, two different true diffusion coefficients and two different levels of a Gaussian white noise ($\sigma = 0.1$ and $\sigma = 0.01$) were chosen in order to generate 1000 trajectories representing the concentration u (measured as profiles of fluorescent level). Using our method of diffusion parameter estimation [14] we obtained 1000 values of D_c for each data set. All these values were statistically processed. Figures 4 and 5 illustrate the results. They are ordered into 4 groups: (i) IC1–IC5 (for $D_T = 0.1$) and $\sigma = 0.01$, (ii) IC1–IC5 (for $D_T = 0.1$) and $\sigma = 0.1$,

(iii) IC6–IC9 (for $D_T = 0.01$) and $\sigma = 0.01$, and (iv) IC6–IC9 (for $D_T = 0.01$) and $\sigma = 0.1$.

The distribution of the squared error $|\frac{D_c - D_T}{D_T}|^2$ is shown in Fig. 4. As we expected according to Tables 1–2, the smallest relative error for $D_T = 0.1$ corresponds the IC1 (an optimal disc, $S_{app} = 949.5$), while for a slower diffusion (for $D = 0.01$) the optimal annulus (IC6, $S_{app} = 485.5$) gives smaller relative error than the optimal disc (IC7, $S_{app} = 307.7$).

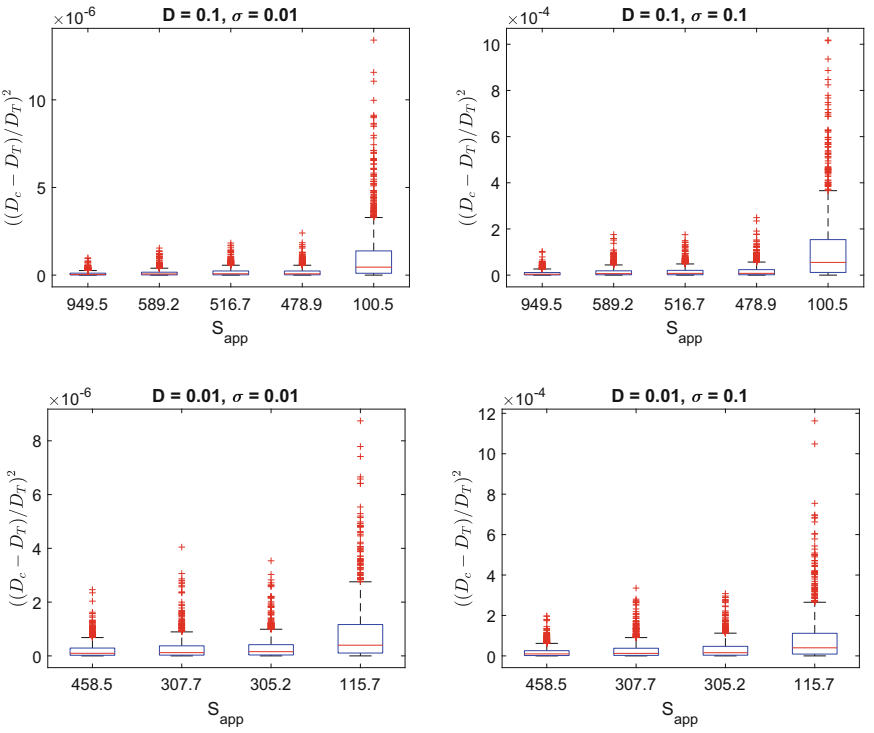

Fig. 4. The results of numerical estimation of diffusion coefficient. The boxplots show the distribution of the squared error $|\frac{D_c - D_T}{D_T}|^2$, each based on 1000 noisy signal samples. The cross marks (+) indicate the outliers. The higher value of S_{app} corresponds to the smaller box (and shorter confidence interval). Note that for both the upper left and right graphical results (for $D = 0.1$) the IC1 (an optimal disc) gives the smallest relative error, while for lower two cases of a slower diffusion (for $D = 0.01$), the optimal annulus (IC6) beats the optimal disc (IC7).

In order to graphically illustrate the difference between theoretically and numerically determined values of the relative error in a diffusion constant estimation, we plotted Fig. 5. It was reached using (7), i.e., the difference $\frac{\sigma^2}{S_{app}} - \mathbb{E}\left(\left|\frac{D_c - D_T}{D_T}\right|^2\right)$ was calculated and consequently statistically processed.

Again, the respective boxplots show these distributions over data sets with different physical (D_T), technical (σ) and experimental (initial conditions IC1–IC9) attributes. The discrepancy is low for all cases, thus, we can rely on our sensitivity based approach to the optimum experiment design. Indeed, we see that the initial condition with maximal value of S_{app} exhibits the narrowest intervals and a distribution that is on average closest to zero than other initial conditions (which confirms the above statement about sensitivity S_{app} based approach).

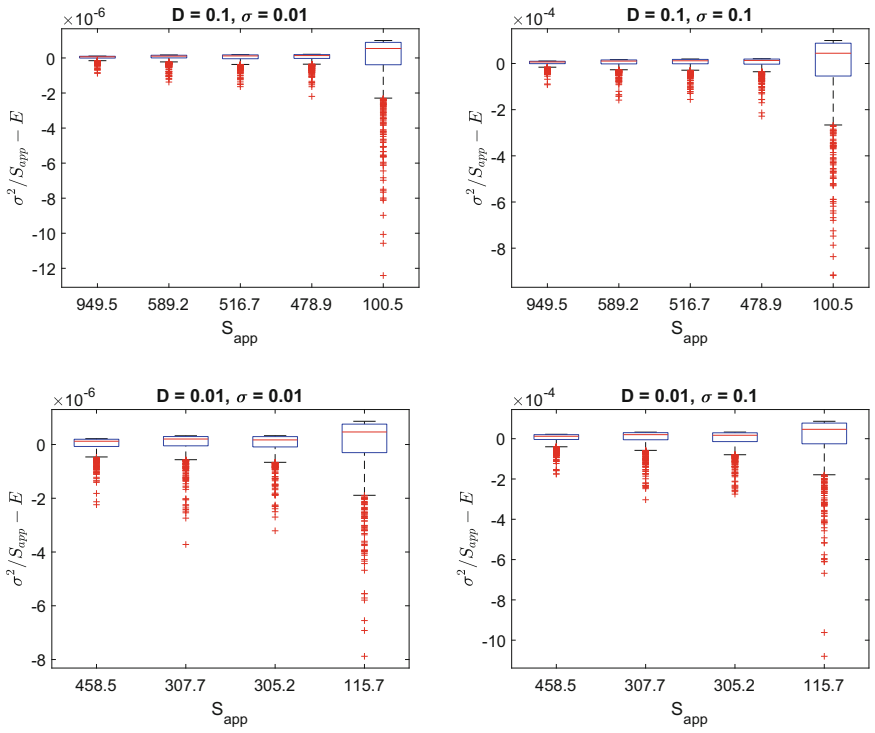

Fig. 5. The graphical results show the difference between the theoretically and numerically determined values of the relative error in a diffusion constant estimation.

Remark 4. Let us add some comments about the solution process of optimization problem (9) and finding the optimal initial condition u_0^{opt}. We used a global optimization method from the UFO system [10]. This method uses local optimization methods for finding local minima. Briefly speaking, we choose an initial $u_0^{(0)} = (1/2, \ldots, 1/2)^T$ and for $k = 0, 1, \ldots$, until the optimality conditions are satisfied, we update the next iterate $u_0^{(k+1)}$ from $u_0^{(k)}$ based on the function value $S_{app}(u_0^{(k)})$ and its gradient. For each D we obtained a solution on the boundary of the feasible region. Thus, $u_0^{opt}(r_i) \in \{1, 0\}$ is a binary-valued vector (there exist non-zero components of u_0^{opt}). As we already explained, a small number

of jumps between 1 and 0 in u_0^{opt} occurs for large values of a scaled diffusion coefficient δ. When δ decreases, the number of jumps increases.

5 Conclusion

In this paper, we have shown the importance of an interconnection between two important activities in performing model based experiments: (i) the setting of experimental factors, and (ii) data processing based on an underlying mathematical model containing the specific experimental conditions as parameters. Although our approach is illustrated on a specific case of photobleaching experiment only, it has general validity. The key concept is based on evaluation of sensitivity of measured data with respect to estimated parameters value. To do so, first we formulated the problem of parameter estimation in precise terms of parameter-to-data map, parameter estimates and their relative errors.

Only after that, our idea of the model-based optimization of experimental conditions was presented on a numerical case study. We set up the numerical procedure leading simultaneously to the optimal size and shape of a bleached domain for which the sensitivity measure reaches the maximal value, hence assuring the smallest relative error of the estimated parameter. Numerical calculations revealed rather surprising results. For high values of the dimensionless diffusion coefficient, the disc is the optimal shape and for smaller values, shapes with more and more components (i.e., annuli-type shapes) become optimal. In particular, this is not the disc which is the best shape, but, for practically relevant values of the experimental settings, sometimes an annulus can be better because it leads to a significant improvement in the confidence interval. Hence, it is proved that the bleach size and shape can be readily optimized and the bleaching pattern represents one of the most important experimental design factors in photobleaching experiments.

We hope that our findings will be incorporated into a novel generation of the FRAP experimental protocols – it is not computationally expensive and the enhancement of the parameter estimation process can be substantial.

Acknowledgement. This work was supported by the long-term strategic development financing of the Institute of Computer Science (RVO:67985807) and by the Ministry of Education, Youth and Sports of the Czech Republic - projects “CENAKVA” (No. CZ.1.05/2.1.00/01.0024), “CENAKVA II” (No. LO1205 under the NPU I program) and ‘The CENAKVA Centre Development’ (No. CZ.1.05/2.1.00/19.0380).

References

1. Bates, D.M., Watts, D.G.: Nonlinear Regression Analysis: Its Applications. Wiley, New York (1988)
2. Blumenthal, D., Goldstien, L., Edidin, M., Gheber, L.A.: Universal approach to FRAP analysis of arbitrary bleaching patterns. Scientific reports 5, Article no. 11655 (2015). https://doi.org/10.1038/srep11655

3. Cintrón-Arias, A., Banks, H.T., Capaldi, A., Lloyd, A.L.: A sensitivity matrix based methodology for inverse problem formulation. J. Inv. Ill-Posed Probl. **17**, 545–564 (2009)
4. Engl, H., Hanke, M., Neubauer, A.: Regularization of Ill-Posed Problems. Kluwer, Dortrecht (1996)
5. Hadamard, J.: Lectures on the Cauchy Problem in Linear Partial Differential Equations. Yale University Press, New Haven (1923)
6. Kaňa, R., Kotabová, E., Lukeš, M., Papáček, Š., Matonoha, C., Liu, L.N., Prášil, O., Mullineaux, C.W.: Phycobilisome mobility and its role in the regulation of light harvesting in red algae. Plant Physiol. **165**, 1618–1631 (2014)
7. Kaňa, R., Matonoha, C., Papáček, Š., Soukup, J.: On estimation of diffusion coefficient based on spatio-temporal FRAP images: an inverse ill-posed problem. In: Chleboun, J., Segeth, K., Šístek, J., Vejchodský, T. (eds.) Programs and Algorithms of Numerical Mathematics 16, pp. 100–111 (2013)
8. Kindermann, S., Papáček, Š.: On data space selection and data processing for parameter identification in a reaction-diffusion model based on FRAP experiments. Abstr. Appl. Anal. Article ID 859849 (2015)
9. Kindermann, S., Papáček, Š.: Optimization of the shape (and topology) of the initial conditions for diffusion parameter identification (2016). https://arxiv.org/pdf/1602.03357.pdf
10. Lukšan, L., Tůma, M., Matonoha, C., Vlček, J., Ramešová, N., Šiška, M., Hartman, J.: UFO 2014 - interactive system for universal functional optimization. Technical report V-1218. Institute of Computer Science, Academy of Sciences of the Czech Republic, Prague (2014). http://www.cs.cas.cz/luksan/ufo.html
11. Mai, J., Trump, S., Ali, R., Schiltz, R.L., Hager, G., Hanke, T., Lehmann, I., Attinger, S.: Are assumptions about the model type necessary in reaction-diffusion modeling? A FRAP application. Biophys. J. **100**(5), 1178–1188 (2011)
12. Mueller, F., Mazza, D., Stasevich, T.J., McNally, J.G.: FRAP and kinetic modeling in the analysis of nuclear protein dynamics: what do we really know? Curr. Opin. Cell Biol. **22**, 1–9 (2010)
13. Mullineaux, C.W., Tobin, M.J., Jones, G.R.: Mobility of photosynthetic complexes in thylakoid membranes. Nature **390**, 421–424 (1997)
14. Papáček, Š., Kaňa, R., Matonoha, C.: Estimation of diffusivity of phycobilisomes on thylakoid membrane based on spatio-temporal FRAP images. Math. Comput. Modell. **57**, 1907–1912 (2013)
15. Papáček, Š., Kindermann, S.: On optimization of FRAP experiments: model-based sensitivity analysis approach. In: Ortuño, F., Rojas, I. (eds.) IWBBIO 2016. LNCS, vol. 9656, pp. 545–556. Springer, Cham (2016). https://doi.org/10.1007/978-3-319-31744-1_49
16. Sadegh Zadeh, K., Montas, H.J., Shirmohammadi, A.: Identification of biomolecule mass transport and binding rate parameters in living cells by inverse modeling. Theor. Biol. Med. Modell. **3**, 36 (2006)
17. Sbalzarini, I.F.: Analysis, modeling and simulation of diffusion processes in cell biology. VDM Verlag Dr. Muller (2009)